



ACCOUNTING FOR MASS TRANSFER KINETICS WHEN MODELING THE
IMPACT OF LOW PERMEABILITY LAYERS IN A GROUNDWATER SOURCE
ZONE ON DISSOLVED CONTAMINANT FATE AND TRANSPORT

THESIS

James M. Bell, Captain, USAF

AFIT-ENV-14-M-08

DEPARTMENT OF THE AIR FORCE
AIR UNIVERSITY

AIR FORCE INSTITUTE OF TECHNOLOGY

Wright-Patterson Air Force Base, Ohio

APPROVED FOR PUBLIC RELEASE; DISTRIBUTION A UNLIMITED

The views expressed in this thesis are those of the author and do not reflect the official policy or position of the United States Air Force, Department of Defense, or the United States Government.

This material is declared a work of the United States Government and is not subject to copyright protection in the United States.

AFIT-ENV-14-M-08

ACCOUNTING FOR MASS TRANSFER KINETICS WHEN MODELING THE
IMPACT OF LOW PERMEABILITY LAYERS IN A GROUNDWATER SOURCE
ZONE ON DISSOLVED CONTAMINANT FATE AND TRANSPORT

THESIS

Presented to the Faculty

Department of Systems Engineering and Management

Graduate School of Engineering and Management

Air Force Institute of Technology

Air University

Air Education and Training Command

In Partial Fulfillment of the Requirements for the
Degree of Master of Science in Engineering Management

James M. Bell, BS

Captain, USAF

March 2014

APPROVED FOR PUBLIC RELEASE; DISTRIBUTION A UNLIMITED

ACCOUNTING FOR MASS TRANSFER KINETICS WHEN MODELING THE
IMPACT OF LOW PERMEABILITY LAYERS IN A GROUNDWATER SOURCE
ZONE ON DISSOLVED CONTAMINANT FATE AND TRANSPORT

James M. Bell, BS
Captain, USAF

Approved:

| | |
|---|-------------|
| <hr/> | <hr/> |
| //signed// | 12 Mar 2014 |
| Mark N. Goltz, Ph. D. (Chairman) | Date |
| <hr/> | <hr/> |
| //signed// | 12 Mar 2014 |
| John D. Christ, Ph. D., Lt Col (Member) | Date |
| USAF | |
| <hr/> | <hr/> |
| //signed// | 12 Mar 2014 |
| Avery H. Demond, Ph. D. (Member) | Date |
| University of Michigan | |
| <hr/> | <hr/> |
| //signed// | 12 Mar 2014 |
| Junqi Huang, Ph. D. (Member) | Date |
| U.S. Environmental Protection Agency | |
| <hr/> | <hr/> |
| //signed// | 12 Mar 2014 |
| Vhance Valencia, Ph. D., Major (Member) | Date |
| USAF | |

Abstract

In this study, the subsurface storage and transport of a Dense Non-Aqueous Phase Liquid (DNAPL), trichloroethylene (TCE), was studied using a numerical model. Poor handling and disposal of chlorinated solvents like TCE have produced numerous DNAPL-contaminated sites that contribute to long term contamination of groundwater. In the subsurface, DNAPLs can pool atop low permeability layers, and despite efforts to remove or destroy the majority of pooled DNAPL, a fraction of the mass can move by diffusion into the low permeability layer and then by back diffusion act as a secondary contamination source for decades. Recent studies have found evidence that cracks can exist in low permeability layers within aquifers. These cracks might be natural or be the result of pooled DNAPL. In either case, the cracks may allow significantly more DNAPL mass to enter the low permeability zones than by diffusion alone. Sievers (2012) developed a model that accounted for the presence of DNAPL in cracked low permeability zones, and found that the resulting dissolved contaminant plume in the high permeability zone could persist for many decades. Sievers (2012) model simulations showed that the rate of mass transfer from the DNAPL phase to the dissolved phase was a critical parameter that controlled plume persistence. While Sievers (2012) modeled the DNAPL dissolution rate as a constant, others have shown the rate is a decreasing function of time. In this research study, we model the DNAPL dissolution rate as both a constant and as a function of time. We apply both models using parameters and conditions applicable to a real world site. This study found that in the case of the time varying rate of mass transfer from the DNAPL to the dissolved phase, because the rate decreases with

time, more DNAPL mass persists in the low permeability zone compared to when the rate is modeled as constant. This results in more persistent dissolved plumes in the high permeability zones, with higher dissolved concentrations. Furthermore, we found that downgradient dissolved contaminant concentrations and mass of DNAPL stored in the low permeability zone as a function of time are very dependent on the parameters used to simulate source dissolution, which further depend on both source and site characteristics, pointing to the need for good source zone characterization.

Acknowledgements

I would like to acknowledge and thank my research advisor, Dr. Mark Goltz for giving me the opportunity to work with him on this research. The guidance, timely edits, and encouragement were vital in the completion of this thesis and greatly appreciated. Dr Junqi Huang at the Robert S. Kerr Environmental Research Center (USEPA) was immensely helpful in the application of the research methods in this thesis. His quick and thorough responses allowed us to quickly identify and solve problems in the model. I would like to thank Dr. John Christ for his guidance and in depth explanations of mass transfer kinetics. I would also like to thank Dr. Avery H. Demond at the University of Michigan for providing guidance and serving as one of my committee members. I would also like to thank the Strategic Environmental Research and Development Program (SERDP) for the funding to make this research possible. Finally, I would like to thank my wife for all of her love and support.

James M. Bell

Table of Contents

| | |
|--|-----|
| Abstract | iii |
| 1. Introduction | 5 |
| 1.1 Background | 5 |
| 1.2 Research Objective | 9 |
| 1.3 Research Questions | 10 |
| 1.4 Research Methodology | 10 |
| 1.5 Scope and Limitations of Research | 11 |
| 1.6 Summary | 12 |
| 2. Literature Review | 13 |
| 2.1 Overview | 13 |
| 2.2 Mass Transfer Kinetics | 16 |
| 2.3 Site Characterization | 21 |
| 2.3.1 Hill Air Force Base Site | 22 |
| 2.3.2 Fort Lewis EGDY Site | 23 |
| 2.3.3 Bachman Road Site | 25 |
| 2.4 Summary | 26 |
| 3. Methodology | 28 |
| 3.1 Overview | 28 |
| 3.4 Site Model | 29 |
| 3.5 Dissolution Kinetics Submodel Implementation | 34 |
| 3.5.1 Assumptions | 35 |
| 3.6 Description of Analyses | 36 |
| 3.7 Summary | 37 |
| 4. Results and Analysis | 38 |
| 4.1 Overview | 38 |
| 4.2 Simulation Results | 38 |
| 4.2.1 Breakthrough Curves | 39 |
| 4.2.2 Mass Analysis | 42 |
| 4.2.3 Sensitivity Analysis | 44 |
| 5. Conclusions and Recommendations | 49 |
| 5.1 Conclusions | 49 |

| | |
|---|----|
| 5.2 Recommendations for future research | 49 |
| Appendix A..... | 52 |
| Bibliography | 54 |

List of Figures

| | |
|---|----|
| Figure 1: Illustration of contaminant movement within subsurface and low permeable matrix (after Kueper & Davies, 2009) | 7 |
| Figure 2: Conceptual Diagram of Contaminant Transport beneath a Source Zone for scenarios 1, 2, 3 (Sievers, 2012) | 14 |
| Figure 3: Bachman Road Site estimated plumes from SEAR study (after Abriola et al, 2005) | 26 |
| Figure 4: Conceptual Model of contaminated aquifer (After Sievers, 2012) | 30 |
| Figure 5: MODFLOW Head Output along a Longitudinal Cross Section (grid blocks are 1m x 1m squares) | 31 |
| Figure 7: Time-Dependent vs Constant Dissolution Rate BTCs (Monitoring Well in Sand) | 39 |
| Figure 8: Time-Dependent vs Constant Dissolution Rate BTCs (Monitoring Well at Sand/Clay Interface) | 40 |
| Figure 9: Time-Dependent vs Constant Dissolution Rate BTCs (Monitoring Well in Clay) | 40 |
| Figure 10: BTCs for Varying β Values (Monitoring Well in Sand) | 46 |
| Figure 11: BTCs for Varying k_{dis} Values (Monitoring Well in Sand) | 47 |

List of Tables

| | |
|---|----|
| Table 1: Fitting Parameter Values (Christ et al., 2006; Parker and Park, 2004, Zhu and Sykes, 2003) | 21 |
| Table 2: Soil layer depths of site at Hill, AFB (Oolman, 1995) | 23 |
| Table 3: Bachman Road Site Hydrogeological Values (Abriola et al., 2005) | 25 |
| Table 4: Parameter Values Input into MODFLOW | 33 |
| Table 5: Parameter Symbols, Definitions, and Values | 35 |
| Table 6: Sensitivity Analysis Values | 37 |
| Table 7: TCE Mass in Low Permeability Zone: Comparison of Two Models | 43 |
| Table 8: Mass Analysis for Sensitivity Analysis | 44 |
| Table 9: Sensitivity Analysis: DNAPL Mass Half lives | 48 |

Accounting for Mass Transfer Kinetics when Modeling the Impact of Low Permeability Layers in a Groundwater Source Zone on Dissolved Contaminant Fate and Transport

1. Introduction

1.1 Background

Chlorinated solvents, like tetrachloroethylene (PCE) and trichloroethylene (TCE), have been widely used as cleaning agents by industry and the Departments of Defense (DOD). Improper disposal of these chemicals has resulted in extensive groundwater contamination. Prior to the institution and enforcement of proper disposal methods, chlorinated solvents were dumped into unlined waste pits, poured down sanitary sewer systems, and partially burned in fire training pits. Poor handling and disposal of chlorinated solvents have produced numerous contaminated sites across DOD and commercial industry. The United States Environmental Protection Agency (EPA) (2013) estimates that over 60% of the sites at which they have mandated cleanup efforts (Superfund sites) are contaminated with chlorinated solvents. The dangers posed by these sites, according to the EPA (2013), are that they can contaminate nearby groundwater and that people who ingest the contaminated water drastically increase their risk for developing liver problems and cancer. The EPA has set the maximum contaminant level (MCL) for TCE in drinking water, the contaminant of interest in this study, at 5 parts per billion, or 5 μ g/L. Chlorinated solvents like TCE, PCE, and 1,1,1-trichloroethane (1,1,1-TCA) are also known as chlorinated aliphatic hydrocarbons

(CAHs). CAHs like TCE have solubility concentrations as high as several g/L, exceeding MCLs by as much as six orders of magnitude.

Chlorinated solvents move down through soils as a dense separate phase immiscible liquid or dense nonaqueous phase liquid (DNAPL) after they are intentionally or accidentally disposed onto the ground. DNAPLs have a specific gravity greater than water; consequently when they reach the water table, they continue to sink in the aquifer. Upon its release into the subsurface, the contaminant moves through the porous media due to gravitational and capillary forces, leaving behind disconnected blobs and small amounts of residual DNAPL, called ganglia. The ganglia can remain in the pore spaces between solids in the aquifer.

DNAPL will also settle as pools on top of lower permeability layers. The DNAPL can dissolve and move by diffusion into the layer over time. Frequently, however, the low permeability layer will be fractured, either naturally or due to the presence of the DNAPL itself (Sievers, 2012). The DNAPL can then move into the fractures, either as a dissolved phase chlorinated aliphatic hydrocarbon (CAH) or as a separate phase DNAPL. For the remainder of this study, we will refer to the dissolved phase as a CAH and the separate phase as a DNAPL. Dissolved and separate phase contaminant in these low permeability layers may function as long lasting contaminant sources, even after the bulk of contamination in the aquifer may have been remediated (AFCEE, 2007). Thus, DNAPL in these low permeability layers can dissolve and diffuse into nearby flowing groundwater, continuing to contaminate downgradient drinking water sources decades after source removal in the overlying aquifer (Sievers, 2012).

Contaminant plume sizes vary according to the initial mass of contaminant present, contaminant properties (e.g., solubility), and aquifer characteristics. Figure 1 shows DNAPL moving into the subsurface, through the higher permeable layers, gathering into pools, and entering the fractures in the low permeability layer.

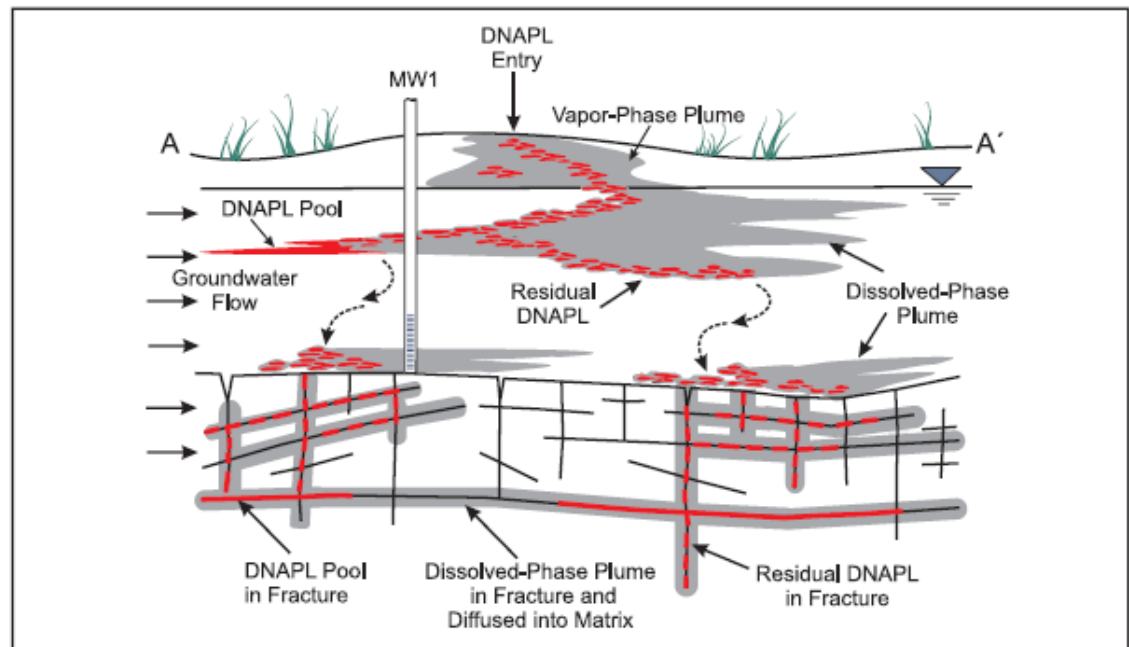


Figure 1: Illustration of contaminant movement within subsurface and low permeable matrix (after Kueper & Davies, 2009)

Often, during source zone remediation multiple technologies are utilized to remove or destroy the DNAPL residual and pools. Typically, these source remediation efforts will focus on DNAPL in high permeability zones. However, technologies that target high permeability zones do not address contaminants that are also found within cracks in the low permeability layers as either a dissolved CAH or a separate phase DNAPL, or in the low permeability matrix itself as a CAH. The contaminant in the low permeability zones can continue to act as a long-term contaminant source, contributing to

contaminant levels well above the MCL, even after remediation of the bulk of contamination in the high permeability zones (Sievers, 2012).

The low permeability layers are typically modeled as competent, homogenous, formations, and transport of contaminant into the layers is modeled as Fickian diffusion. The diffusion coefficient in Fick's law accounts for the tortuosity of the low permeability layer and retardation due to contaminant sorption in the solid particles within the layer (Parker et al., 2008). Recently, however, the applicability of this Fickian model has been questioned, and the potential for enhanced transport in these low permeability layer is being studied (Sievers, 2012).

An ongoing Strategic Environmental Research and Development Program (SERDP) project is investigating the impact of DNAPL contamination in low permeability layers on contaminant plume evolution and persistence (Demond, 2010). In particular, the research project is focused upon the effect of cracks (both naturally occurring and due to the presence of the DNAPL pool itself) in the low permeability zone on the dissolved contaminant plume. As part of the research project, a team at the University of Michigan is conducting experimental studies to investigate the formation of cracks due to the presence of a DNAPL pool, as well as the diffusive transport of dissolved contaminant into the low permeability layers. Also, as part of the SERDP study, Sievers (2012) investigated the characteristics and occurrence of naturally occurring cracks. Sievers (2012) developed a model to assess the impact of DNAPL transport into a cracked low permeability zone on plume persistence and found that the rate of mass transfer of DNAPL from the cracks into the dissolved phase was a critical

process that affected dissolved plume longevity. For simplicity, Sievers (2012) modeled the rate of mass transfer using a constant first-order rate coefficient. However, other research has shown that the mass transfer coefficient changes with time (Christ et al., 2006; Zhu and Sykes, 2003; Parker and Park, 2004). Given the significance of the mass transfer rate on plume evolution and persistence, as was found by Sievers (2012), an important research endeavor would be to develop a realistic model of mass transfer from the DNAPL to the dissolved phase as a function of time, and simulate its effect on dissolved plume evolution and persistence.

1.2 Research Objective

The primary objective of this research is to gain a better understanding of CAH plume evolution and persistence. This goal will be approached by attempting to model how the rate of mass transfer from DNAPL in cracked low permeability layers to the dissolved phase changes over time. Given the importance of the rate of DNAPL mass transfer on dissolved plume evolution and persistence, this research effort will attempt to better simulate DNAPL mass transfer kinetics. Sievers (2012) developed a model that simulated DNAPL in cracked low permeability layers, with dissolution of the DNAPL governed by first-order kinetics with a constant first-order rate coefficient. In the current study, this model will be extended to more realistically allow the DNAPL mass transfer kinetics to vary in time. The model will be analyzed by applying it to a real world site using literature values.

1.3 Research Questions

1. How is the down gradient concentration vs. time (breakthrough) different for the two models (constant mass transfer rate coefficient vs. a mass transfer coefficient that's a function of time)?
2. For realistic site conditions, how long will significant down gradient contaminant concentrations persist after DNAPL removal from an aquifer, if DNAPL is not removed from the low permeability layer underlying the aquifer?
3. What model parameters cause the down gradient contaminant plume concentration to change the most; that is what parameter has the greatest impact on contaminant down gradient concentration?

1.4 Research Methodology

1. A literature review will be conducted to determine (1) the various sub models that may be used to simulate the change in DNAPL mass transfer coefficient with time, and (2) hydrogeological and contaminant characteristics of "typical" sites that have DNAPL pools atop low permeability layers.
2. Based upon the literature review, an appropriate time dependent mass transfer sub model will be chosen and incorporated into the Sievers (2012) model. A comparison of down gradient contaminant plume concentration versus time (breakthrough) curves will be simulated by the two models (constant mass transfer rate coefficient vs. a mass transfer coefficient that's a function of time).

3. The model will be applied using realistic site data obtained from the literature review of “typical” sites, to simulate contaminant plume evolution and persistence resulting from DNAPL in cracked low permeability layers.
4. A sensitivity analysis will be conducted by changing parameter values and analyzing results to determine what parameters have the most impact on down gradient contaminant plume concentrations.

1.5 Scope and Limitations of Research

The modeling performed in this research explores highly idealized systems to examine the possible impact of the mass transfer coefficient on subsurface plume evolution. The model developed in this study is to be used to help us gain a qualitative understanding of DNAPL plume behavior, not as a tool to predict contaminant concentration distribution at any particular site. The values for simulations are based on common values and trends found in the literature. This model makes assumptions similar to those made in Sievers (2012) study: (1) no degradation or sorption of the contaminant, (2) the subsurface material properties in each layer are homogeneous with respect to space and time, (3) steady state flow, and (4) the effect of vertical cracking in the low permeability layer on flow can be effectively simulated by an increase in vertical hydraulic conductivity. This research study will use GMS modeling software, modified to account for mass transfer dissolution kinetics varying with time.

1.6 Summary

Past disposal practices have led to groundwater contamination by chlorinated solvents. These solvents have been shown to cause cancer, liver problems, and other harmful effects when ingested by humans. Remediation efforts have attempted to remove these chemicals from the soil at numerous contaminated locations; however they remain at many sites. Although remediation technologies may be successful in removing contaminant mass from highly permeable zones, it has proved difficult to address contamination in low permeability zones. In particular, modeling by Sievers (2012) has demonstrated that cracks in these low permeability zones may allow storage of a significant mass of DNAPL, resulting in contamination levels in plumes of dissolved CAH above MCLs for decades. In her study, Sievers (2012) found the DNAPL dissolution rate, which she assumed was constant over time, to be a controlling parameter when modeling the persistence of down gradient contaminant concentrations. Other researchers have modeled the DNAPL dissolution rate as a function of time (Christ et al., 2006; Parker and Park, 2004; Clement et al, 2004; Zhu and Sykes, 2003). In this research effort, we will modify the Sievers (2012) model to incorporate a DNAPL mass transfer rate that varies with time and apply the modified model using parameters and conditions applicable to a real world site. In the following section, we review literature dealing with DNAPL dissolution kinetics. We also investigate real world sites that may be applicable (based upon our model assumptions) for use as case studies for us to simulate. .

2. Literature Review

2.1 Overview

This section presents literature on previous research efforts relevant to DNAPL dissolution mass transfer kinetics. Studies of DNAPL contaminated sites which might be appropriate to model are also reviewed. Understanding the processes that govern contaminant transport in an aquifer is crucial in setting and achieving remediation goals to reduce risks associated with CAH-contaminated groundwater. As discussed earlier, gravity forces move DNAPL down through porous media until it forms pools atop low permeability layers. Non-wetting DNAPLs can move through large pores in higher permeability areas and into cracks existing in lower permeability layers or bedrock (Kueper & Davies, 2009). Pools of DNAPL can dissolve into flowing groundwater, diffuse into the low permeability matrix, enter cracks in the low permeability zone as DNAPL and ultimately create plumes extending from the source zone that can spread for miles. Miniter (2011) modeled the diffusion of a DNAPL source into a low permeability layer using 3D numerical simulations with the DoD Groundwater Modeling System (GMS). He used GMS as a tool to analyze how cracks in the layer impact the longevity of the dissolved phase CAH plume. Miniter's research yielded results that indicate the presence of cracks support "enhanced diffusion" (Miniter, 2011). The results of his model showed that increased cracking allowed greater amounts of contaminant mass to enter the low permeability clay layer. The increased mass led to greater diffusion out of the clay resulting in higher downgradient plume contaminant concentrations, even after the source was removed (Miniter, 2011).

Sievers (2012) used literature values to vary crack geometry and spacing to compare models in three scenarios: (1) CAH diffusion into an uncracked low permeability clay layer; (2) CAH advection-dispersion into cracks with diffusion into the clay matrix, and (3) separate phase DNAPL movement into the cracks followed by diffusion into the clay matrix. Figure 2 shows a conceptual diagram for the contaminant transport in each scenario.

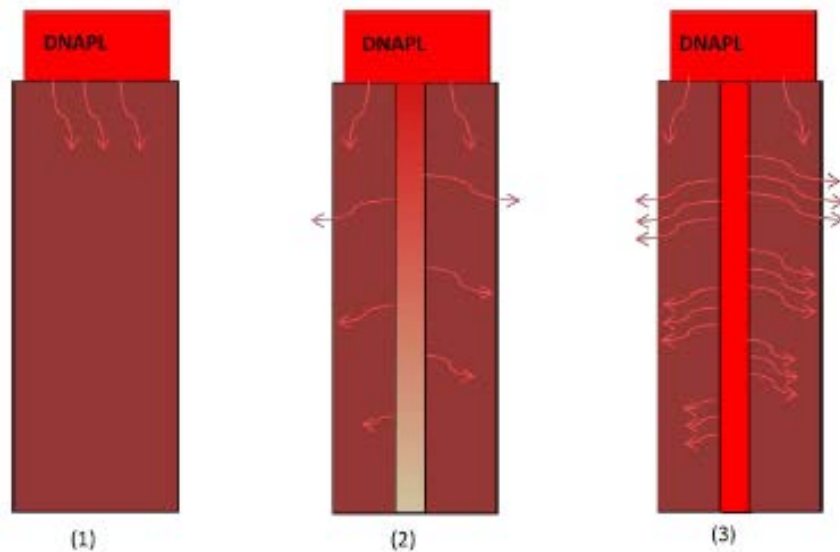


Figure 2: Conceptual Diagram of Contaminant Transport beneath a Source Zone for scenarios 1, 2, 3 (Sievers, 2012)

Sievers modeled the evolution and persistence of the contaminant downgradient as a result of back diffusion out of the clay layer and into flowing groundwater. The downgradient concentrations she found were well above MCL concentrations for decades. Cracking was found to significantly contribute to downgradient concentrations. Sievers also found that the CAH downgradient concentrations are highly dependent on the rate of DNAPL dissolution. For simplicity, she modeled the dissolution rate as a constant. As discussed in the following section, Christ et al. (2006), Parker and Park

(2004), Clement et al (2004), and Zhu and Sykes (2003) model the mass transfer rate or rate of dissolution as a function of time. Given the importance of the dissolution rate, this research effort will attempt to adopt a time-dependent dissolution rate model from the literature and incorporate it into Sievers' model to simulate plume evolution

Mass transfer from a DNAPL in stagnant water is described by Fick's Law. According to Fick's First Law, solute is transported from regions of high concentration to low concentration with a flux (mass per area per time) that is proportional to the concentration gradient. The rate of mass transfer can be increased if the water is not stagnant (resulting in higher concentration gradients) or when there is increased contact area between the water and the DNAPL.

Correlations have been developed to account for the effect of groundwater velocity and DNAPL saturation on the mass transfer rate (Nambi and Powers, 2001). Simulations run by Sievers (2012) showed that the rate of mass transfer, which was quantified in her model by a first-order rate constant, is very important to CAH plume evolution and persistence. This is not surprising, as the mass transfer rate constant quantifies the rate at which contaminant dissolves from the nonaqueous phase to the aqueous phase. In her research, Sievers (2012) assumed that DNAPL remains in the low permeability zone after a DNAPL pool has been removed from the high permeability zone. Over time, the DNAPL dissolves into the pore water that surrounds it in the low permeability zone matrix. Then, by back diffusion, CAH is transferred from the low permeability zone to the high permeability zone. In this way, DNAPL in the low permeability zone serves as a long-term source of contaminant, resulting in dissolved

concentrations of CAH in the high permeability aquifer that persist for decades (Sievers, 2012). In her simulations, Sievers (2012) found that the rate of mass transfer from the DNAPL to the surrounding pore water, which she assumed was constant, was a critical parameter that determined the longevity of the contaminant plume in the aquifer. In fact, research has shown that the rate of mass transfer from a DNAPL varies over time, as the DNAPL dissolves and its architecture changes (Parker et al., 1994). In the sections that follow we will review literature that accounts for how the rate of mass transfer from a DNAPL varies, as DNAPL architecture changes over time.

2.2 Mass Transfer Kinetics

Mass transfer kinetics can be defined as the rate at which mass moves from one phase to another. In DNAPL-contaminated groundwater, we are primarily concerned with the rate of dissolution from the DNAPL phase to the dissolved CAH phase.

Zhu and Sykes (2003), Parker and Park (2004), Clement et al. (2004), and Christ et al. (2006) employ an effective mass transfer coefficient that changes over time to account for mass transfer kinetics. The effective mass transfer coefficient accounts for mass transfer processes averaged over the entire DNAPL source volume. A common method used by researchers to account for the complexities of mass transfer in a contaminated aquifer, which is affected by spatial variations of the DNAPL architecture and the hydrogeological conditions, is to apply an upscaled mass transfer function (MTF) (Zhu and Sykes, 2003; Parker and Park, 2004; Clement et al., 2004; Christ et al., 2006). The MTF represents the various processes that affect mass transfer and which vary in space by a single spatially-averaged expression. MTF parameters, although usually site

specific, are “capable of accurately describing field-scale DNAPL dissolution rates as a function of time” (Parker and Park, 2004).

Clement et al. (2004) developed a mathematical model to analyze groundwater contaminant fate and transport in a system with a DNAPL source. In the work, mathematical equations were programmed into a reactive transport code called RT3D (Clement et al., 2004). RT3D is a component of GMS (Sievers, 2012). RT3D employs an advection, dispersion equation with a first-order mass transfer term to describe dissolution of a contaminant from a DNAPL source. Equation 2.1 shows the basic advection, dispersion equation with the added mass transfer term (Clement et al., 2004)

$$\frac{\partial C}{\partial t} = \frac{\partial}{\partial x_i} \left(D_{ij} \frac{\partial C}{\partial x_j} \right) - \frac{\partial}{\partial x_i} (v_i C) + k_L a (C^* - C) \mp F \quad (2.1)$$

where C is the aqueous-phase concentration of the DNAPL contaminant [ML^{-3}], C^* is the equilibrium aqueous phase concentration (solubility) of the contaminant [ML^{-3}], D is the hydrodynamic dispersion coefficient [L^2T^{-1}], v is the pore water velocity [LT^{-1}], $k_L a$ is the DNAPL dissolution rate constant [T^{-1}] and the factor F represents all other physical, bio/geo-chemical reactions [$ML^{-3}T^{-1}$]. The model assumes the DNAPL is immobile and has a negligible effect on aquifer porosity and hydrodynamic conductivity (Clement et al, 2004). These assumptions are valid at low DNAPL saturation levels (Zhu and Sykes, 2003). Parameters like F and $k_L a$ in equation 2.1 are commonly used in hydrological research to describe physical and chemical phenomena (like degradation or sorption). We will refer to these parameters as phenomenological factors from time to time in this study. The F parameter is not used in this study because as previously

mentioned, we assume no degradation or sorption. $k_L a$ is the overall first-order mass transfer rate with units of $[T^{-1}]$. a is the specific surface area $[L^2 L^{-3}]$ and $k_L [LT^{-1}]$ is a mass transport coefficient. The specific surface area (a) is of interest in this study because as discussed earlier, an increase in the contact area between the water and DNAPL can increase the overall mass transfer rate.

Clement et al. (2004) use equation 2.2 to compute the DNAPL dissolution rate, $k_L a$:

$$k_L a = k_L^{max} a \left(\frac{M(t)}{M_0} \right)^\beta \quad (2.2)$$

where $k_L^{max} a$ is the maximum dissolution rate constant at time zero, which is a function of the porous medium and DNAPL characteristics, β is an empirical constant, M_0 is the initial mass of the DNAPL in the sediments, and $M(t)$ is the mass of DNAPL in the sediments at time t . Clement et. al (2004) tested differing values of k_L^{max} in their model. They found that higher values of k_L^{max} result in increased downgradient concentrations within their model. Equation 2.2 is the first of four mass transfer models that will be introduced in this chapter.

Three additional mass transfer models from the literature are discussed in the following sections. All three models are similar, though they were formulated with varying notations. In this work, the notation for the various models has been made consistent, to minimize confusion when comparing the models.

Parker and Park (2004) implemented three dimensional numerical experiments to model field-scale DNAPL dissolution kinetics with an MTF. The MTF is shown in Equation 2.3.

$$K_{eff} = K_o' \left(\frac{\bar{q}}{\bar{K}_s} \right)^\alpha \left(\frac{M}{M_0} \right)^\beta \quad (2.3)$$

Note that K_{eff} is the first-order mass transfer rate for contaminant dissolving from the DNAPL to the aqueous phase, and is equivalent to $k_L a$ in equation 2.1. The terms in Equation 2.3 are defined by Parker and Park (2004) as follows: \bar{K}_s is the effective saturated hydraulic conductivity [LT^{-1}], \bar{q} is the average Darcy velocity [LT^{-1}], M_0 is the initial DNAPL mass [M], M is the DNAPL mass [M] at time, t , and K_o' [T^{-1}], α [-], and β [-] are model parameters. The α parameter is equal to a value of 1 in all of Parker and Park's (2004) simulations. The β and K_o' values used in their research effort can be found and compared with the parameters of the other models discussed in this section (Table 1).

Zhu and Sykes (2003) utilized one dimensional column simulations to develop three simple screening models that account for mass transfer kinetics. The third and most complicated model, which they labeled NL2, accounts for the change in the rate of DNAPL dissolution with time. Equation 2.4 represents the NL2 model

$$\frac{C_0(t)}{C_s} = K_o' \left(\frac{M(t)}{M_0} \right)^\beta \quad (2.4)$$

where $C_0(t)$ is the dissolved contaminant concentration [ML^{-3}] in the water adjacent to the DNAPL at a given time, t , C_s is the contaminant solubility [ML^{-3}], K_o' [-] is a parameter that indicates at time zero how far the dissolved contaminant concentration is from equilibrium (*i.e.*, solubility), $\frac{M(t)}{M_0}$ [-] is the fraction of NAPL mass remaining at a given time, and β [-] is a fitting parameter. Note that this model calculates the mass

transfer rate implicitly; there is no mass transfer rate constant explicitly calculated, as in the previous models that have been presented.

According to Christ et al. (2006) all upscaled mass transfer correlations have the same basic form shown in Equation 2.5 below:

$$K_{eff} = K'_0 \left(\frac{M(t)}{M_0} \right)^\beta \quad (2.5)$$

Where K'_0 [d^{-1}] and β [-] are fitting parameters and $\frac{M(t)}{M_0}$ is the fraction of NAPL mass remaining at a given time. As mentioned earlier, K_{eff} is the DNAPL dissolution rate; it equates to $k_L a$ in equation 2.1. The K'_0 and β parameters can be thought of as phenomenological factors that are used to model how the rate of mass transfer changes with time. β may be thought of as a constant that accounts for the heterogeneity of the DNAPL source (Christ, 2014). K'_0 accounts for mixing and dilution “as water flows through the nonuniform DNAPL saturation distribution” (Christ et al., 2006). As explained by Christ et al., (2006), the DNAPL dissolution rate decreases over the life of a site because the high surface area globules and ganglia dissolve quickly, leaving behind persistent pools of DNAPL that dissolve more slowly. Despite their theoretical attractiveness and simplicity, as explained by Christ et al. (2006), the use of upscaled models is limited to site specific parameters. The values of K'_0 and β in the Christ et al. (2006) work were based on the Bachman Road Site. The value of β is provided in Table 1 and can be compared with the other models discussed in this section.

Table 1: Fitting Parameter Values (Christ et al., 2006; Parker and Park, 2004, Zhu and Sykes, 2003)

| Reference | System Description | K'_0 (day^{-1}) | β |
|--------------------------|--|---|---|
| Christ et. al. (2006) | Sixteen 3-D numerical simulations based on Bachman Road Site | 8.2×10^{-3} | 0.85 |
| Zhu and Sykes (2003) | 1-D column system using nonlinear model NL2 | NA(1) | 1.31 |
| Parker and Park (2004) | 3-D simulation of DNAPL dissolution in upper, lower, and combination of both regions | Upper: 4.9×10^{-4} Lower: 2.4×10^{-5} Combination: 4.9×10^{-4} | Upper: 1.10 Lower: 0.40 Combination: 1.40 |

(1) The K'_0 in Zhu and Sykes (2003) is dimensionless

As seen in Table 1, the values for K'_0 and β differ significantly between models because the parameter values are highly dependent on source and site characteristics. For example, the Zhu and Sykes (2003) parameter values were based on one dimensional column simulations as opposed to the parameter values based on the Bachman Road Site in the work by Christ et al. (2006). Huang (2013) implements Equation 2.5 as a subroutine in RT3D (Clement et al., 2004). The subroutine is discussed further in Chapter 3.

2.3 Site Characterization

Aquifers are generally heterogeneous. They can consist of different materials to include: cracked rock, cobbles, gravel, sand, clay, and silt. Consequently, site characterization is important when modeling contaminant transport since the geologic structure of an aquifer will control the speed and direction of contaminant movement. In this section, we will look in the literature to find well-characterized real world DNAPL-

contaminated sites relevant to the model's assumptions. As discussed earlier, our model assumes the presence of a pooled DNAPL sitting atop a cracked low permeability layer. Quality site characterization data are essential to the development of a groundwater contamination model (Sale & McWhorter, 2001). Source zone architecture has also been determined to be a key factor governing transport (Christ et al., 2006). Christ et al. (2006) evaluate the efficacy of numerous groundwater contamination model efforts using multiphase numerical simulations and support Sale & McWhorter's (2001) findings regarding the importance of site and source characterization, stating the "future improvement of the predictive capability of upscaled mass transfer models will likely require incorporation of additional site-specific information" (Christ et al., 2006).

Three real world contamination sites that have DNAPL pools atop low permeability layers were identified in the literature. The following sections introduce the sites.

2.3.1 Hill Air Force Base Site

Between the years 1967 and 1975 degreasing solvents were dumped into two sandy unlined disposal pits at Hill Air Force Base located near Layton, Utah. Oolman et al. (1995) characterize the aquifer hydrogeology with borehole data readings from 150 locations. The contaminant was reported to consist of trichloroethylene (TCE) and other chlorinated solvents. The unlined pits are located atop a thick clay aquiclude and the contaminant has dissolved to form an approximately 1000 meters long plume. The aquifer in question is composed of silt, sand, gravel, and clay occurring at irregular intervals at various depths (Oolman et al., 1995). The clay aquitard below the aquifer

was also reported to be heterogeneous in nature with intermittent layers of sand and silt. Table 2 provides the approximate depths of soil layers determined from one of the well borings at Hill AFB (Oolman et al., 1995).

Table 2: Soil layer depths of site at Hill, AFB (Oolman, 1995)

| Soil Material | Depth of each layer (m) |
|----------------------|--------------------------------|
| Silt | 3 |
| Silty Sand | 2.5 |
| Sand and Gravel | 3 |
| Clay | Boundary Layer |

The hydraulic conductivities in the sand layers were reported by Oolman et al. (1995) to range from 1.73 m/d to 10.37 m/d.

2.3.2 Fort Lewis EGDY Site

According to the EPA's Superfund Record of Decision (ROD) document (1990), the East Gate Disposal Yard (EGDY) site is located at the Fort Lewis Military Reservation near Tacoma, Washington. The site was part of the Fort Lewis Logistics Center built in 1940. The center and was used for storing supplies and maintaining military equipment and vehicles. The EGDY site was used to dispose of solvents and oils in 24 excavated trenches from 1946 to 1960. Brooks et al. (2008) conducted site characterization at the EGDY site in an effort to measure contaminant fluxes for remediation efforts that include pump and treat methods, thermal remediation, and passive monitoring. They found that the contaminant source was predominantly made up

of TCE and other chemical solvents. TCE concentrations near the source area range from 0.5 to more than 50 mg/l. The concentrations in the plume are reported by the EPA (1998) to range from 0.1 to 0.2 mg/l. The source of contaminant subsequently produced a plume that is estimated to reach up to 4000 meters. The EPA (EPA Superfund Explanation of Significant Differences, 1998) reports that “the time required (to remediate the site) will be considerably longer than 78 years”. The aquifer at the EGDY site is described as “consisting of loose, well-graded, sandy, cobbly gravel or gravelly sand...underlain by a (less permeable) layer consisting of loose to dense silty, sandy gravel with some clay” (Brooks et al, 2008). They found that the media under this aquitard consists of more sand and gravel combined with stone. Although the site is well characterized, the depths of each soil layer were not found in the literature; probably due to the high degree of heterogeneity at the site as the EPA reports that “the hydrostratigraphy of the area is quite complex” (EPA EGDY ROD, 1990). The water table at the EGDY site is reported by the EPA Superfund ROD (1990) to be between 7 to 35 feet below the surface and groundwater moves at an average velocity of 3feet per day.

2.3.3 Bachman Road Site

The Bachman Road site is located in Oscoda, Michigan near a former dry cleaning facility less than 250 feet west of Lake Huron as shown on Figure 3. The site was well characterized in research performed as part of a pilot-scale surfactant enhanced aquifer remediation (SEAR) effort conducted by Abriola et al. (2005). The site is described by Abriola et al. (2005) as a “sandy glacial outwash.” It consists of approximately eight meters of sand atop a confining clay layer. Table 3 provides hydrogeological data associated with the Bachman Road site (Abriola et al, 2005).

Table 3: Bachman Road Site Hydrogeological Values (Abriola et al., 2005)

| Hydrogeological attribute | Value (units) |
|---|----------------|
| Sand Layer | 8 (m) |
| Clay Layer | Boundary Layer |
| Mean Hydraulic Conductivity of the Sand | 16.8 (m/d) |
| Mean porosity | 0.36 |

As previously discussed, Christ et al. (2006) conducted an analysis of DNAPL dissolution kinetics that was based on the Bachman Road Site. Figure 3 provides a visual layout of the contamination plumes and monitoring well locations used to characterize the Bachman Road site in the SEAR study.

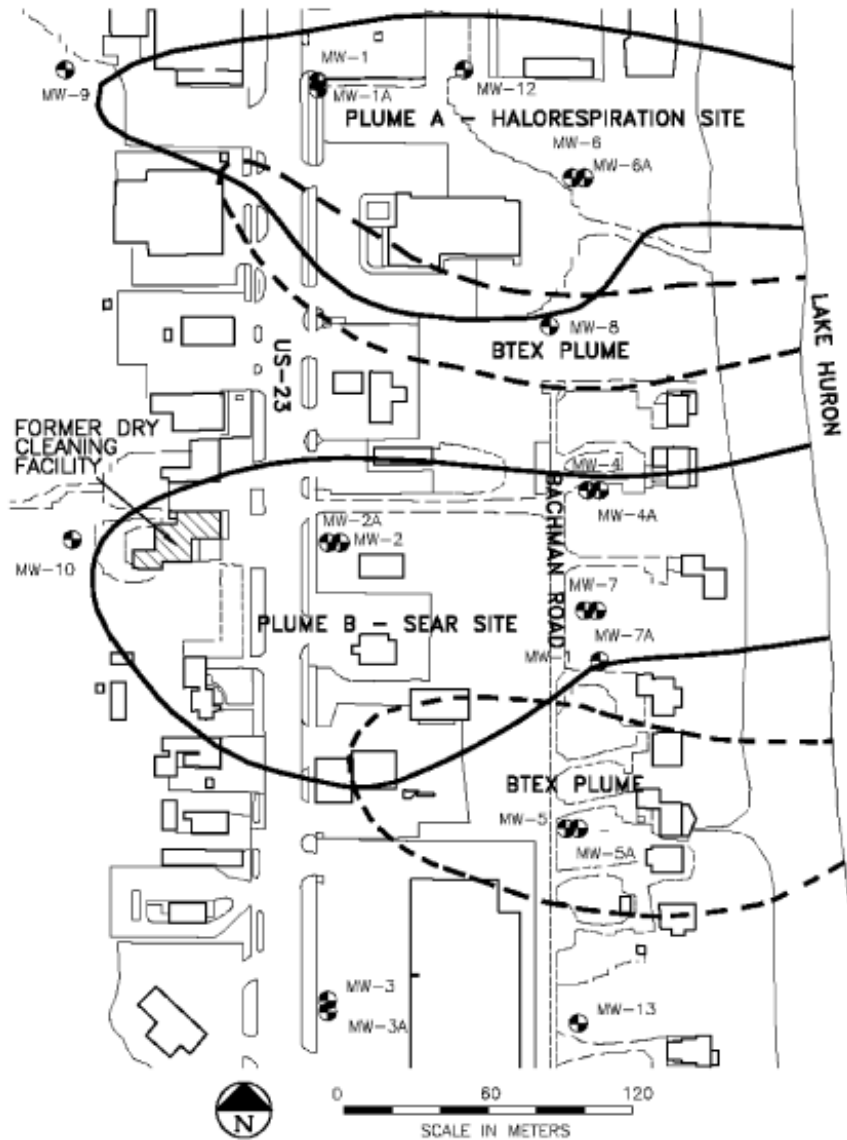


Figure 3: Bachman Road Site estimated plumes from SEAR study (after Abriola et al, 2005)

2.4 Summary

Minter (2011) found that the presence of cracks support enhanced diffusion to allow greater contaminant mass to enter low permeability layers. Sievers (2012) continued the research and produced results that indicate the presence of DNAPL in cracks within low permeability layers can support contaminant concentrations well above MCLs decades after remediation has removed the contaminant source from high permeability zones. Sievers (2012) also found that the rate of mass transfer significantly affects contaminant fate and transport. She modeled the mass transfer rate as a constant for simplicity. However, Zhu and Sykes (2003), Parker and Park (2004), Clement et al. (2004), and Christ et al. (2006) modeled mass transfer as a function of time. Each model in the research takes on a similar mathematical form; however, the mass transfer parameter values differ significantly, based upon the different site and DNAPL source characteristics that are being simulated. Given that the model parameter values are dependent on site characteristics, the characteristics of three real-world contaminant sites are assessed for their potential use as model scenarios.

In the following chapter, a contaminant site is selected and a model, which incorporates time-varying DNAPL dissolution kinetics, is built to simulate plume genesis and evolution at the site. Such an approach will allow us to observe how time-varying DNAPL dissolution kinetics may affect dissolved contaminant plume behavior using a model that incorporates parameters based upon a real-world scenario.

3. Methodology

3.1 Overview

This work is an extension of the research performed by Sievers (2012). The Sievers' model, which assumed the transfer rate for mass dissolution from the DNAPL was constant, is modified to allow for time varying mass transfer. Results of the new model will be compared to results of the Sievers' model, using parameter values that are based on a real world site.

Christ et al. (2006) developed a basic MTF model to simulate DNAPL dissolution, using parameters based on the Bachman Road Site. The Christ et al. (2006) study was focused on DNAPL dissolution kinetics, and did not consider the impact of the dissolution process on plume evolution at the site. In the current study, we will incorporate a DNAPL dissolution sub model into a larger model of the Bachman Road site, to investigate the impact of a time-dependent dissolution rate constant on plume evolution. The fact that Christ et al. (2006) based their parameter values on the Bachman Road site, and that the site itself has been well-characterized, leads us to choose that site for this modeling study. In this study we will be conducting three operations with the chosen model. We will use the parameter values of Christ et al. (2006) in conjunction with the Huang (2013) submodel to (1) simulate concentration versus time plots, known as breakthrough curves (BTCs) downgradient of a DNAPL source, (2) track DNAPL mass and dissolved mass in the aquifer over time, and (3) conduct sensitivity analyses. Each operation is discussed further in following sections.

3.4 Site Model

This section describes the model that was built using the Groundwater Modeling System (GMS) software. Two modeling packages within GMS were employed in this study, MODFLOW (Chapman and Parker, 2011) and RT3D (Clement et al., 2004). GMS was used to create a numerical grid that simulates the real-world contaminated aquifer at the Bachman Road Site. The depth of the three dimensional numerical grid was developed based on the aquifer depth at the Bachman Road Site (Abriola et al., 2005). The simulated aquifer in this work has a length of 70 meters (m), a width of 70 m, and a depth of 14 m. The mean hydraulic conductivity, mean porosity, and the depths of the soil layers from the Bachman Road Site are used in the site model. The Bachman Road Site hydrogeological data can be found in Table 3. Each cell in the grid represents a cube with sides of 1 m. The simulated high permeability sand layer is 8 m thick atop a 4 meter thick low permeability clay layer. The clay zone overlays a 2 m high permeability sand layer to avoid having a no-flow boundary condition at the bottom of the clay layer (Sievers, 2012). Layers 1-8 are sand, 9-14 are a mix of clay and cracked clay, and 15-16 are sand. A $16m^2$ cracked clay zone is simulated in the low permeability layer. The source zone was located above the cracked clay. Figure 4 shows a conceptual model of the DNAPL pool sitting atop the cracked low permeability zone.

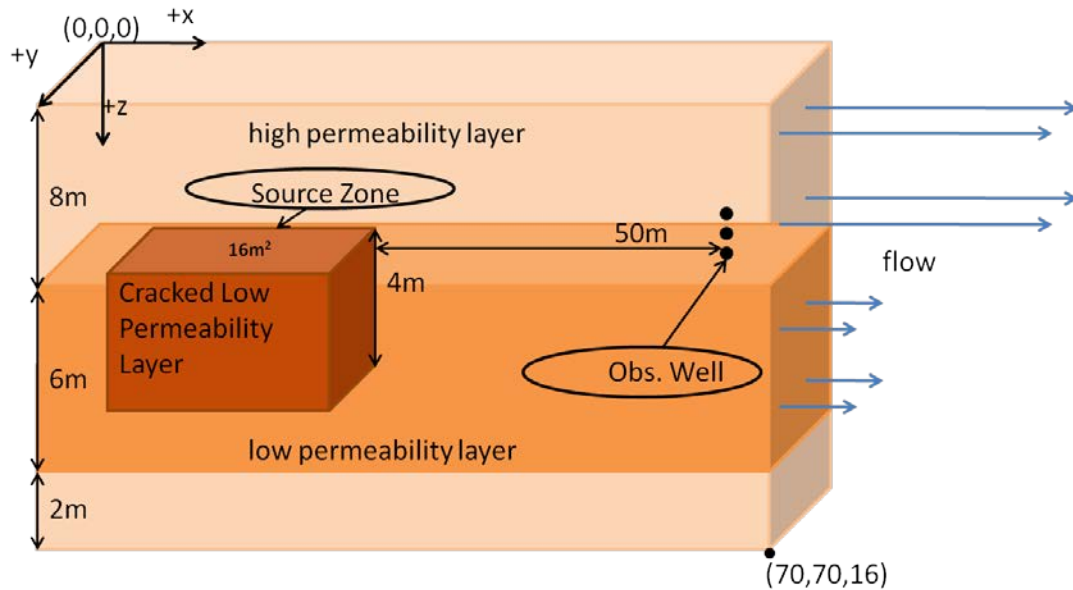


Figure 4: Conceptual Model of contaminated aquifer (After Sievers, 2012)

As shown in Figure 4, three monitoring wells were placed 50m down gradient from the source to measure concentrations at a location in the plume over time. The well locations are in the sand, interface, and clay layers, respectively. The locations of the source zone can be seen as orange circles and the monitoring wells can be seen as black circles in Figure 5. The cracked clay zone was placed directly under the source zone. The location can be seen in Figure 5 as a brown box. Figure 5 was output by MODFLOW and shows the hydraulic heads throughout the model domain. MODFLOW calculates

these heads assuming steady state flow and based on the specified boundary conditions.

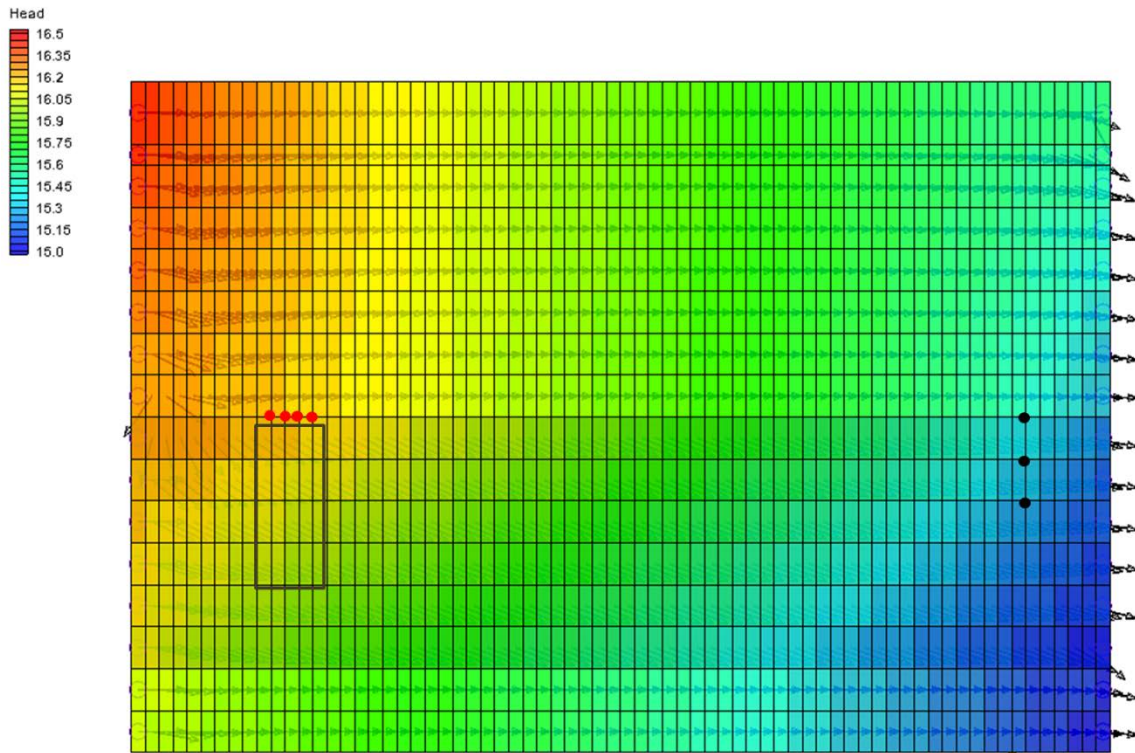


Figure 5: MODFLOW Head Output along a Longitudinal Cross Section (grid blocks are 1m x 1m squares)

The aquifer is assumed to be unconfined, and a horizontal hydraulic gradient of 1m/70m was established by setting the head at the left and right boundaries of the domain at 16.5 and 15.5m, respectively. A vertical hydraulic gradient of .5m/16m was established by setting the bottom heads at the left and right hand boundaries to 16m and 15m, respectively. The gradients allowed water to flow from top to bottom and left to right. Flow is from high head to low head. The flow vectors can be seen as arrows in Figure 5. The MODFLOW flow velocities are used as input by the RT3D code.

RT3D models advection, dispersion, and diffusion of the contaminant throughout the domain. The total simulation was run for two periods, totaling 50 years. A $16m^2$ DNAPL pool was modeled by establishing constant concentration cells for an initial 10 year period (Figures 4 and 5). A constant concentration of 110 mg/l was used for the source (Sievers, 2012). After the first 10 years, the source was assumed to be remediated, and the constant concentration cells were removed. Contaminant from the source was transported into and out of the low permeability layer by diffusion and advection. Especially in the cracked clay, advection in the low permeability zone could be significant. Although individual cracks were not explicitly modeled, the cracked clay is modeled by increasing the vertical conductivity within the low permeability zone. The simulation was run for 40 years after remediation to analyze DNAPL dissolution and the effect of back diffusion on down gradient plume concentrations in the aquifer. Values of the vertical and horizontal hydraulic conductivity, longitudinal dispersivity, and porosity were assigned to the sand, clay and cracked clay (Sievers, 2012). The parameter values input into MODFLOW are shown in Table 4.

Table 4: Parameter Values Input into MODFLOW

| Media | Sand | Clay | Cracked Clay |
|--------------------------------|-------|---------|--------------|
| Horizontal $K_h [\frac{m}{d}]$ | 17.28 | 4.32E-5 | 4.32E-5 |
| Vertical $K_v [\frac{m}{d}]$ | 1.728 | 4.32E-6 | 4.32E-4 |
| Longitudinal Dispersivity [m] | 1.0 | 1.0E-4 | 1.0E-4 |
| Porosity [θ] | 0.35 | 0.43 | 0.487 |

For this study we assumed the cracks in the source zone were 90% saturated with DNAPL and 10% saturated with water. Since modeling the individual cracks proved infeasible, we approximated the cracked low permeability zone as an equivalent porous media with a high vertical hydraulic conductivity (Table 4) with a DNAPL saturation equivalent to 90% DNAPL in the cracks “smeared” throughout the cracked low permeability zone. The equivalent DNAPL saturation was 6.62E-5 (Sievers, 2012). Sievers (2012) can be seen for a detailed description of crack formation and modeling. The initial DNAPL saturation was set to 6.62E-5 at times 0 and 10 years, as that value equates to 90% saturation in the cracks. The reason the saturation is “reset” to 6.62E-5 after 10 years is because the model simulates that the saturation declines between years 0 and 10 (as the DNAPL dissolves). However, in the conceptual model, the DNAPL pool sitting atop the cracked clay constantly replenishes DNAPL in the cracks for the first 10 years of the simulation, before the pool is remediated at year 10. Thus, at year 10, the saturation in the cracked clay zone is reset to its initial value, to simulate this constant replenishment of DNAPL into the cracks.

3.5 Dissolution Kinetics Submodel Implementation

Huang (2013) incorporated a sub model to simulate DNAPL dissolution kinetics into the RT3D code (Clement et al., 2004). The sub model is based on Equation 2.5 presented in Christ et al. (2006). Since RT3D tracks NAPL saturation, rather than mass, Huang (2013) converted the masses in Equation 3.1 to their equivalent saturations:

$$k_{eff} = K'_o \left(\frac{M(t)}{M_o} \right)^\beta = K'_o \left(\frac{V \rho_{NAPL} S_{NAPL}}{V \rho_{NAPL} S_o} \right)^\beta \quad (3.1)$$

where V is the volume of DNAPL [L^3], ρ_{NAPL} is the density of the DNAPL [ML^{-3}], S_{NAPL} is the saturation of DNAPL [L^3 DNAPL per L^3 aquifer], and S_o is the initial saturation of DNAPL [-]. Rewriting Equation 3.1:

$$k_{eff} = K'_o \left(\frac{S_{NAPL}}{S_o} \right)^\beta = \frac{K'_o}{S_o^\beta} (S_{NAPL})^\beta \quad (3.2)$$

The time-dependent dissolution sub model formulated by Huang (2013) therefore, is based on tracking the DNAPL saturation over time. The rate constant for dissolution is k_{dis} , defined in equation 3.3.

$$\frac{K'_o}{S_o^\beta} = k_{dis} \quad (3.3)$$

This rate decreases over time, based on the value of β . For the values of β and K'_o used by Christ et al. (2006) to simulate dissolution at the Bachman Site, 0.85 and $8.2E-3$ [day^{-1}], respectively (see Table 1) and the initial DNAPL saturation in the cracks assumed by Sievers (2012) of 0.9, the resulting value of k_{dis} is $8.97E-3$ [day^{-1}].

The sub model developed by Huang (2013) requires the user to define six parameter values associated with the contaminant and media. The parameters and their values are listed in Table 5.

Table 5: Parameter Symbols, Definitions, and Values

| Parameter Symbol | Parameter Definition | Parameter Value |
|------------------|---|-------------------------------------|
| ρ_β | Bulk density of the media | 1.46E6 [mg/l] |
| α | Mass transfer coefficient for rate-limited adsorption | 0 [day ⁻¹] |
| β | Dissolution sub model exponent | $8.5E - 1^{(1)}$; $8.5E - 5^{(2)}$ |
| C_S : | Solubility of TCE in Water | 1100.0 [mg/l] |
| k_{dis} | Dissolution sub model rate constant | 8.97E-3 [day ⁻¹] |
| k_d | Partition coefficient of adsorption | 0 [kg ⁻¹] |

(1) (Christ et al., 2006)

(2) β was set to near zero to simulate a constant mass transfer rate

Sorption is not examined in this study; consequently the adsorption parameters α and k_d are set equal to zero.

3.5.1 Assumptions

Numerous assumptions are required when modeling contaminant fate and transport in an aquifer. The subsurface is generally known to be anisotropic and heterogeneous. This results in significantly different flows at different points within the same medium. The model in this research effort assumes each zone is homogeneous and isotropic; in other words we assume the same hydraulic and chemical properties in each media zone. Instantaneous removal of the source was assumed to simulate complete remediation of the DNAPL mass in the high permeability sand layer. This study employs many of the same assumptions listed in the research performed by Sievers (2012). For a

detailed explanation of the assumptions used in the cracked clay zone consult the work of Sievers (2012). Many of the governing equations used in this research are the same equations used in the work performed by Minitier (2011). The work of Minitier (2011) can be consulted for further explanation of the governing equations.

3.6 Description of Analyses

As previously discussed, the model developed in this study was used for three types of analyses: (1) to simulate concentration versus time plots, known as breakthrough curves (BTCs), at locations downgradient of a DNAPL source, (2) to quantify DNAPL mass and dissolved mass in the low permeability zone as a function of time, and (3) to conduct sensitivity analyses.

BTCs can give us information such as when concentrations drop below certain levels or how much of an impact certain parameters have on contaminant concentrations over time. In this study, the BTCs are used to compare two models, a constant dissolution rate model as opposed to a time-dependent dissolution rate model.

The GMS model outputs may be used to track DNAPL mass and dissolved mass in various zones. Of particular interest in this study is the mass within the low permeability zone, as that serves as the long-term contamination source. It is also of interest to compare how the simulations of the constant dissolution rate model and the time-dependent dissolution rate model compare, with respect to the simulated DNAPL mass as a function of time.

The purpose of the sensitivity analysis was to elicit which parameters have the most impact on simulated contaminant fate and transport. While Sievers (2012) found

that the rate of DNAPL dissolution was an important parameter affecting contaminant fate and transport, the current study hones in on the two parameters that describe the dissolution rate; β and k_{dis} . Table 6 presents the baseline and sensitivity analysis values.

Table 6: Sensitivity Analysis Values

| Parameter | Lower Sensitivity Analysis Value | Baseline Value | Upper Sensitivity Analysis Value |
|--------------------------------|---|-----------------------|---|
| β [–] | 8.5E-5 | 8.5E-3 | 8.5E-1 |
| k_{dis} [day ⁻¹] | 8.97E-3 | 8.97E-1 | 89.7 |

3.7 Summary

The Bachman Road site was chosen for analysis in this study. A model which included both time-dependent and constant DNAPL dissolution rates was formulated and incorporated into RT3D within GMS. The model was implemented based on the characteristics of the Bachman Road site (Abriola et al., 2005) and the mass transfer model developed by Christ et al. (2006). In Chapter 4, we will present and discuss the results of the model simulations.

4. Results and Analysis

4.1 Overview

The results of the model described in chapter 3 are presented in the following sections. Simulations include concentration vs time breakthrough curves (BTCs) at downgradient monitoring wells to compare the difference in results of the time-dependent dissolution rate and constant dissolution rate sub models. The results also show differences in mass storage over time, as well as a sensitivity analysis that allows us to determine which parameters most influence downgradient concentrations.

4.2 Simulation Results

The data and figures shown in this section are presented for two sub models: (1) a constant mass transfer rate function and (2) a time-dependent mass transfer rate. The BTCs plot concentration against time for a total simulation period of 50 years. Figure 7, Figure 8, and Figure 9 in the following section plot the concentrations at the observation points in the sand, clay/sand interface, and clay media zones, respectively, when the mass transfer parameter (β) was set equal to $8.5\text{E-}5$ [-] to simulate a constant dissolution rate (see Equation 3.2) compared to when the mass transfer parameter was set equal to $8.5\text{E-}1$ [-] to simulate a time-dependent rate. As previously discussed, the EPA has set the maximum contaminant level (MCL) for TCE in drinking water, the contaminant of interest in this study, at 5 parts per billion, or $5\mu\text{g/L}$. The MCL is shown on each figure to compare with the simulated downgradient concentrations.

4.2.1 Breakthrough Curves

The three breakthrough curves (BTCs) shown below (Figures 7, 8, and 9) plot concentration versus time over 50 years (or 18250 days). All three of the following figures show the BTCs at observation wells simulated by a constant dissolution rate model compared with BTCs simulated by a time-dependent dissolution rate model. All wells are located 50m downgradient from the source zone. Figures 7, 8, and 9 show the BTCs for wells located in the sand, sand/clay interface, and clay, respectively. Note that the clay layer contains the cracked clay source zone.

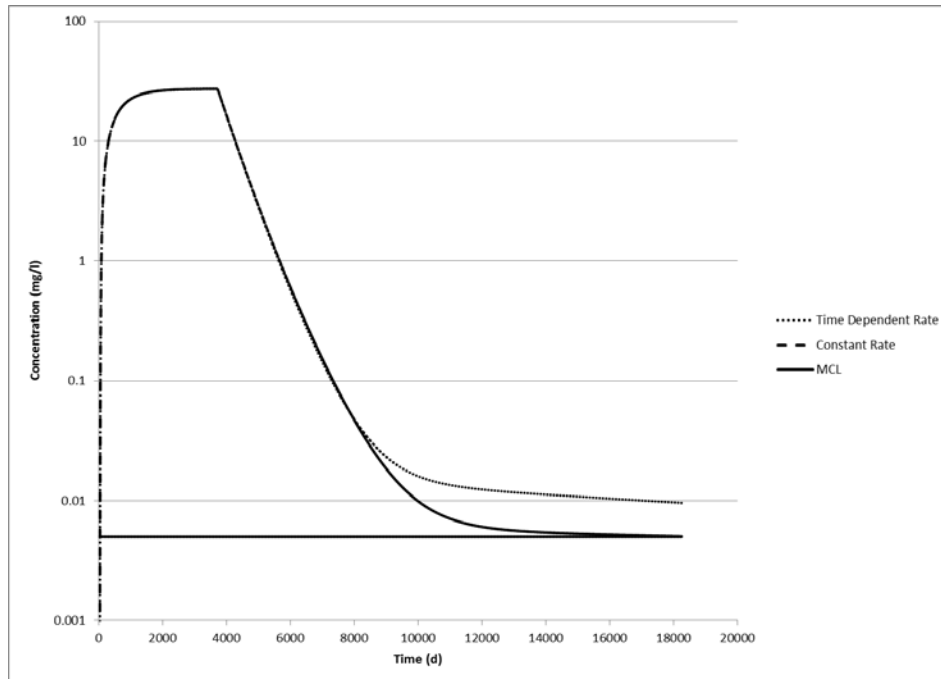


Figure 6: Time-Dependent vs Constant Dissolution Rate BTCs (Monitoring Well in Sand)

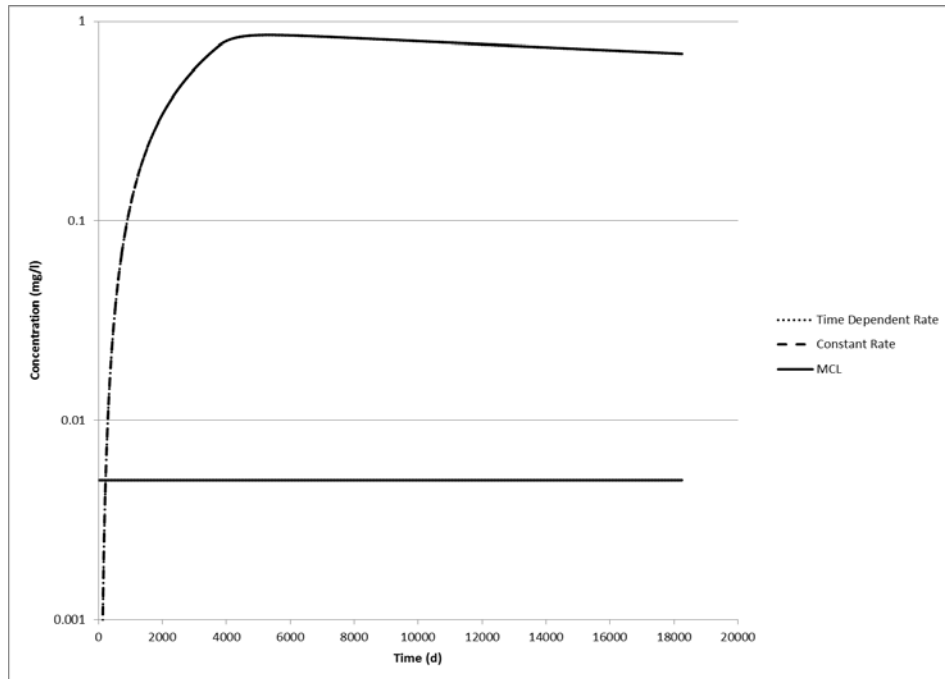


Figure 7: Time-Dependent vs Constant Dissolution Rate BTCs (Monitoring Well at Sand/Clay Interface)

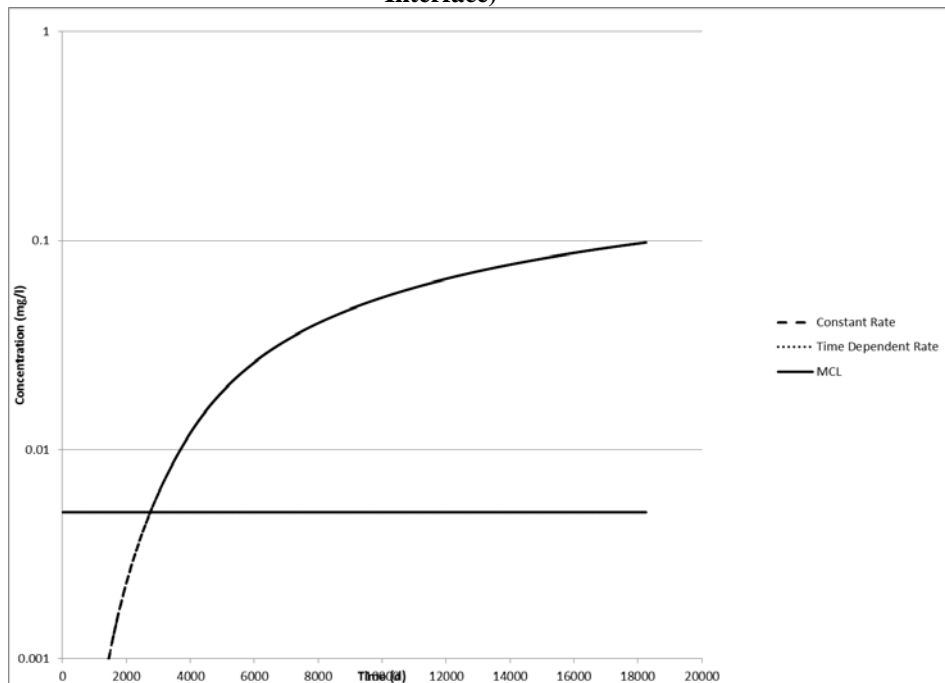


Figure 8: Time-Dependent vs Constant Dissolution Rate BTCs (Monitoring Well in Clay)

Qualitatively, the BTCs display behavior we would expect. The concentrations increase rather quickly in the higher permeability sand zone as seen in Figure 7. The concentrations then rapidly decrease after the source is removed, followed by tailing caused by back diffusion. As expected, the increase in concentration was much slower at the monitoring well in the clay zone (Figure 9) than at the wells in either the sand (Figure 7) or sand/clay interface (Figure 8) due to the small advective transport of dissolved TCE into the clay.

These results are similar to Sievers' (2012) work; the concentration in the sand layer dropped below the MCL after several years and the concentration in the clay and at the interface remain above the MCL for over forty years after remediation. The concentration in the clay media zone continues to increase after the 50 year simulation is complete. A longer term simulation (data not shown) indicated that after sixty years the concentrations in the low permeability clay began to decrease. Total mass in the clay layer reduces extremely slowly, because in addition to back diffusion, which allows mass to leave the low permeability clay, a fraction of the contaminant mass continues over time to diffuse deeper within the clay. As seen in Figure 7, the time-dependent and constant rate model BTCs begin to diverge after about 8000 days (approximately 20 years). The time-dependent BTC has a thicker tail, indicating more persistent concentrations above the MCL than simulated by the constant rate model. This is due to the fact that the constant rate model simulates higher dissolution rates than the time-dependent rate model. As we will see in the next section, the slower dissolution rates simulated by the time-dependent model result in DNAPL mass remaining in the low

permeability zone for a longer time than simulated by the constant rate model, and this mass is the source that contributes to the tail that we see in Figure 7. In Figures 8 and 9, we note that there is no difference in the BTCs simulated by the two models for the monitoring wells in the clay or at the sand/clay interface.

4.2.2 Mass Analysis

The purpose of the mass analysis is to quantify the amount of contaminant stored in the low permeability layer over time. The times of interest are at the start of the simulation at 0 years, after removal of the source at 10 years, and at the end of the simulation at 50 years. As previously discussed, at 10 years, the DNAPL in the cracked clay source zone is renewed. This simulates our conceptual model, which has pooled DNAPL atop the cracked clay continually transporting DNAPL into the cracks over the initial 10 year period, before the source is removed. During this time, since the model doesn't include DNAPL transport, the DNAPL saturation is reduced. To account for the presence of the pool feeding DNAPL into the cracks for the initial 10 years, at the 10 year point, the DNAPL saturation in the cracked clay is reset to the initial saturation. The contaminant stored in the low permeability zone acts as a secondary long term source, back diffusing contaminant long after the primary source is removed through remediation. Consequently, the mass of this secondary source is important to quantify. Note that simulation results indicate that the majority of mass is stored at the top of the clay layer. For example, at 50 years, the time-dependent dissolution model simulates that over 75% of the total mass in the low permeability zone was found in the top layer. Table 7 shows the calculated mass in the low permeability clay layer at 0, 10, and 50

years for the time-dependent dissolution rate model compared with the constant dissolution rate model.

Table 7: TCE Mass in Low Permeability Zone: Comparison of Two Models

| Constant Dissolution Rate Model | | | | Time-Dependent Dissolution Rate Model | | | |
|---------------------------------|---------|----------|----------|---------------------------------------|---------|----------|----------|
| | 0 years | 10 Years | 50 Years | | 0 Years | 10 Years | 50 Years |
| Mass (kg) | | | | Mass (kg) | | | |
| Dissolved TCE | 0 | 20.4 | 1.65 | Dissolved TCE | 0 | 20.1 | 0.83 |
| DNAPL TCE | 6.18 | 6.18 | 0 | DNAPL TCE | 6.18 | 6.18 | 3.41 |
| Total Mass | 6.18 | 26.6 | 1.65 | Total Mass | 6.18 | 26.3 | 4.24 |

The dissolved TCE mass at 10 years and 50 years simulated by the constant dissolution rate model is more than the mass simulated by the time-dependent dissolution rate model. At 50 years, nearly twice as much dissolved TCE was observed in the constant dissolution rate model simulation as the time-dependent model simulation. The higher aqueous concentrations seen when the dissolution rate is constant are due to the fact that while the rate of dissolution decreases over time with the time-dependent dissolution rate model, the constant rate model maintains a higher rate of DNAPL dissolution over the course of the simulation. This can also be seen by looking at the DNAPL mass simulations. All of the DNAPL mass is simulated to be dissolved in 50 years using the constant dissolution rate model. This is in contrast to more than half of the DNAPL TCE mass still remaining after 50 years, as simulated by the time-dependent dissolution rate model.

The simulation was rerun to determine when the DNAPL mass was reduced to 50% of the initial mass (at the 10 year point) in both models. The DNAPL mass for the time-dependent rate model is reduced to roughly 50% of the initial mass 52 years after the saturation levels were reset at the 10 year point (results are also shown in Table 9 of the following section). In contrast, the DNAPL mass for the constant rate model is reduced to 50% of the initial mass 2 years after the saturation levels were reset. From these results, we see that assuming a constant dissolution rate is a very non-conservative assumption with regard to remediation time.

The mass table results in conjunction with the BTC analysis indicate that the time-dependent rate model predicts more DNAPL remaining in the low permeability zone for a longer time, resulting in a longer-term source, and more tailing, as compared to when the dissolution rate is constant. This is due to the fact that the time-dependent model simulates slower dissolution rates than the constant rate model.

4.2.3 Sensitivity Analysis

Table 8 shows the simulated mass distribution in the low permeability zone for the sensitivity analysis.

Table 8: Mass Analysis for Sensitivity Analysis

| | $\beta = 8.50E - 5^{(1)}$ | | | $\beta = 8.50E - 3^{(1)}$ | | | $\beta = 8.50E - 1^{(1)}$ | | |
|---------------------|---------------------------|--------|--------|---------------------------|--------|--------|---------------------------|--------|--------|
| | 0 yrs | 10 yrs | 50 yrs | 0 yrs | 10 yrs | 50 yrs | 0 yrs | 10 yrs | 50 yrs |
| Dissolved TCE (kg) | 0 | 20.4 | 1.65 | 0 | 20.3 | 1.35 | 0 | 20.1 | 1.30 |
| DNAPL TCE (kg) | 6.18 | 6.18 | 0 | 6.18 | 6.18 | 2.74 | 6.18 | 6.18 | 3.41 |
| Total Mass TCE (kg) | 6.18 | 26.6 | 1.65 | 6.18 | 28.9 | 4.75 | 6.18 | 26.3 | 4.24 |

(1) The k_{dis} value used for all Beta sensitivity mass simulations was $8.97E-3 \text{ [day}^{-1}\text{]}$

| | $k_{dis} = 8.97E - 5 [days^{-1}]^{(2)}$ | | | $k_{dis} = 8.97E - 3 [days^{-1}]^{(2)}$ | | | $k_{dis} = 8.97E - 1 [days^{-1}]^{(2)}$ | | |
|---------------------|---|--------|--------|---|--------|--------|---|--------|--------|
| | 0 yrs | 10 yrs | 50 yrs | 0 yrs | 10 yrs | 50 yrs | 0 yrs | 10 yrs | 50 yrs |
| Dissolved TCE (kg) | 0 | 22.0 | 1.28 | 0 | 20.1 | 1.30 | 0 | 22.7 | 2.3 |
| DNAPL TCE (kg) | 6.18 | 6.18 | 6.18 | 6.18 | 6.18 | 3.41 | 6.18 | 6.18 | 0 |
| Total Mass TCE (kg) | 6.18 | 28.2 | 7.46 | 6.18 | 26.3 | 4.24 | 6.18 | 28.9 | 2.3 |

(2) The β value used for all k_{dis} sensitivity mass simulations was $8.50E-1[-]$

Table 8 shows how the k_{dis} [day⁻¹] and $\beta[-]$ parameters govern DNAPL dissolution kinetics. As seen in the top table, after 50 years, the mass of DNAPL increases and the mass of dissolved TCE decreases as the value of $\beta[-]$ increases. This is because the higher the value of $\beta[-]$, the more the dissolution rate decreases over time, which results in less dissolved TCE and more DNAPL TCE.

The response to increasing values of k_{dis} shown in the bottom of Table 8 is similar. The larger the value of k_{dis} , the faster the dissolution, resulting in less DNAPL mass remaining and more dissolved mass at a given time.

The following figures show BTCs at observation points located 50m downgradient from the source. Figure 10 shows all three BTCs for β values ranging from $8.5E-1$ to $8.5E-5$ in the sand media zone.

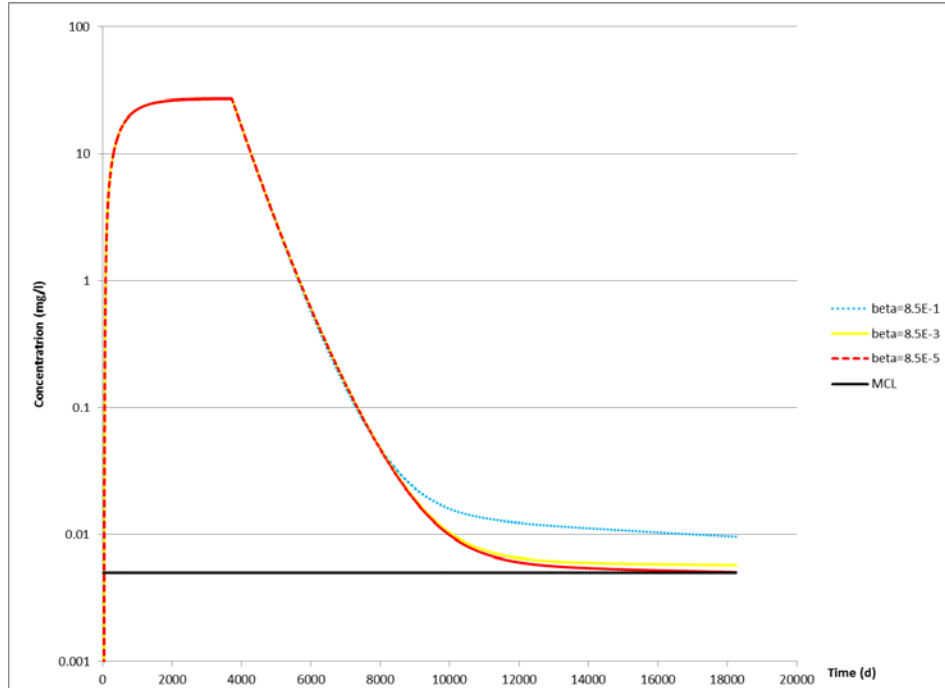


Figure 9: BTCs for Varying β Values (Monitoring Well in Sand)

No significant difference is seen in the model simulations for wells located in the Clay and Sand/Clay interface zones for varying values of β [-], so those figures are not shown. Figure 10 indicates that the tailing in the sand layer increases as the value of β increases. This is consistent with the earlier observations that showed that as β increases, there is a larger decrease in the dissolution rate over time, leading to more DNAPL mass remaining in the low permeability zone and more tailing.

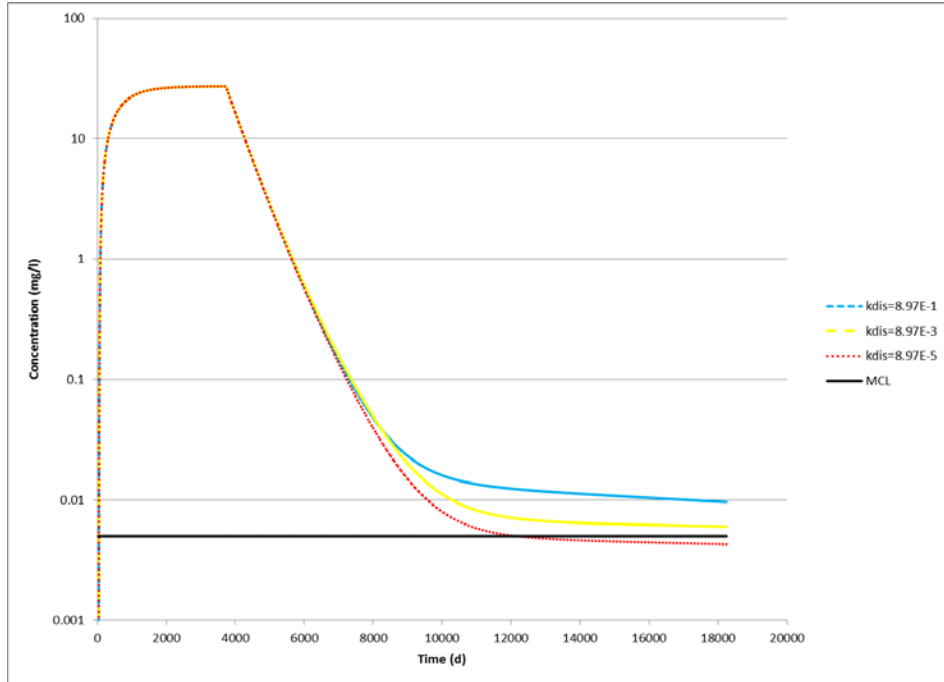


Figure 10: BTCs for Varying k_{dis} Values (Monitoring Well in Sand)

Similarly, Figure 11 shows that higher values of k_{dis} result in higher dissolved concentrations over a 50 year period. A longer term simulation (data not shown) indicated that after 95 years the higher k_{dis} BTC dipped below the other BTCs. This result agrees with the mass values in Table 8 which show no DNAPL is left to feed the high k_{dis} BTC at 50 years. No significant difference is seen in the model simulation for wells located in the clay and sand/clay interface zones, so those results are not shown.

Table 9 lists the time in years when the DNAPL source has been reduced to 50% of its 10 year value for different values of β and k_{dis} . For this study, we designate the time required to reduce the DNAPL mass to 50% of its initial mass as the half-life. To understand Table 9, recall that in order to simulate our conceptual model, at 10 years the DNAPL saturation was reset to its initial saturation value. The half lives listed in Table 9

indicate the time between the 10 year point, when saturation was reset, and the time at which the DNAPL mass was reduced to half of its initial value.

Table 9: Sensitivity Analysis: DNAPL Mass Half Lives

| β Values [-] ⁽¹⁾ | Time (yrs) | k_{dis} Values [$days^{-1}$] ⁽²⁾ | Time (yrs) |
|-----------------------------------|------------|---|------------|
| $8.50E - 5$ | 2 | $8.97E - 5$ | 90+ |
| $8.50E - 3$ | 21 | $8.97E - 3$ | 52 |
| $8.50E - 1$ | 52 | $8.97E - 1$ | 1 |

(1) The k_{dis} value used for all Beta mass half-life simulations was $8.97E-3$ [day^{-1}](2) The β value used for all k_{dis} mass half-life simulations was $8.50E-1$ [-]

Table 9 shows that as β increases, there is an increase in the half-life and as k_{dis} increases, the half-life decreases. Note that after 90 years for the very low k_{dis} value of $8.97E-5$ [$days^{-1}$], only 10% of the initial DNAPL mass had dissolved, so we can reasonably speculate that it would take several more decades for the DNAPL to be reduced by 50%, even though β is low. Table 9 is consistent with the previous analysis of the BTCs and mass tables.

5. Conclusions and Recommendations

5.1 Conclusions

This research examined the effect of mass transfer kinetics as a function of time on downgradient concentrations at a real world site. Previous research has shown that the DNAPL dissolution rate is time-dependent, with the rate decreasing as a function of time. The analysis of mass distribution and BTCs showed that when the dissolution rate is time dependent; the mass of DNAPL that persists in the low permeability zone remains larger over time as compared to when the rate is modeled as a constant. The persistent DNAPL mass results in more persistent dissolved plumes in high permeability zones, with higher dissolved concentrations. Assuming a constant dissolution rate is a very non-conservative assumption with regard to remediation time. If one assumes the rate is time-dependent rate, as past research would suggest, the half-life of the DNAPL source is increased by several decades. In the case of cracked low permeability zones, this finding means that significantly more contaminant mass can reside in the cracks for a longer time when the dissolution rate is time-dependent as opposed to when it to be constant.

5.2 Recommendations for future research

The assumptions and limitations of this study provide opportunities for future research. For example, this research assumes no degradation or sorption of the dissolved contaminant. The RT3D code developed by Clement et al. (2004) can account for both

sorption and degradation. A model that accounts for these processes would provide more realistic results. In addition, as discussed below, considering these processes, along with consideration of simulated mass discharge, could help with development of better management strategies for DNAPL contaminated sites. to The current approach used by the EPA to manage contaminated sites is to compare the contaminant concentrations measured at the site with the MCL. This approach results in costly and lengthy cleanups to meet strict drinking water standards.

The EPA is considering adoption of a “flexible approach to setting remedial objectives” (InsideEPA.com, 2013). This is important, because the findings of this study, along with other (Sievers, 2012; Minitier, 2011) indicate that effective remediation will fail to decrease contaminant concentrations below the MCL for over 40 years, suggesting lengthy and costly cleanups for contaminated sites. In fact, “estimates by the EPA (in 2004) indicate that expenditures for soil and groundwater cleanup at over 300,000 sites through 2033 may exceed \$200 billion...and many of these sites have experienced groundwater impacts” (NRC, 2012). One approach that has been proposed as a remedy is to base site management decisions on flux or mass discharge measurements, rather than concentration measurements. Mass discharge quantifies the contaminant mass being transported by the groundwater per unit time (ITRC, 2010).

The model developed in this study could easily be used to simulate mass discharge and flux data. These data could be used to determine if the mass discharge from the source is low enough for other attenuation processes (like degradation or sorption) to be considered protective. A modeling effort that incorporates sorption,

degradation, and mass discharge would provide realistic and relevant results for environmental regulators and researchers alike.

Appendix A

Definitions

Advection - Flow resulting from an externally applied pressure difference or from gravity/density changes

Chlorinated Aliphatic Hydrocarbon (CAH) – Term used in this research for dissolved phase DNAPL

Dense Non Aqueous Phase Liquid (DNAPL) – A fluid with a density greater than water which is relatively immiscible in water

Diffusion – Movement of dissolved solute governed by a concentration gradient according to Fick's Law

Dispersion – The process in which solute mixing occurs during advective transport caused by the velocity variations
Dissolution – The process of dissolving (e.g., from a DNAPL phase to a dissolved phase)

Enhanced Diffusion – Increased diffusion in a low permeability porous medium due to the presence of cracks in the medium
Hydraulic Conductivity – The capacity of a medium to transmit water

Globule–A small round particle (or drop) of a substance

Maximum Contaminant Level (MCL) – Legal limit for a contaminant in drinking water as established by the Environmental Protection Agency

Permeability – The measure of ease in which fluid moves through porous material

Sorption – The binding of a contaminant to porous media

Upscaled Model – A macroscopic, effective, or field scale domain averaged model that incorporates the effects of spatial variations in DNAPL saturations and flow through a source zone by using a mass transfer coefficient (Christ, 2006)

Wettability – the affinity of the DNAPL for a solid surface in the presence of water

Definition of Units

In this research effort, when defining variables in equations the units will follow the variable in brackets. The units shown below will be used.

F-Force

L-Length

M-Mass

T-Time

Bibliography

Abriola, L. M., Drummond, C. D., Hahn, E. J., Hayes, K. F., Kibbey, T. C. G., Lemke, L. D., . . . Rathfelder, K. M. (2005). Pilot-scale demonstration of surfactant-enhanced PCE solubilization at the bachman road site. 1. site characterization and test design. *Environmental Science & Technology*, 39(6), 1778-1790. doi:10.1021/es0495819

AFCEE, Air Force Center for Engineering and the Environment. *AFCEE Source Zone Initiative Final Report*. Brooks AF Base: US Air Force, 2007.

Brooks, M. C., Wood, A. L., Annable, M. D., Hatfield, K., Cho, J., Holbert, C., . . . Smith, R. E. (2008). Changes in contaminant mass discharge from DNAPL source mass depletion: Evaluation at two field sites. *Journal of Contaminant Hydrology*, 102(1–2), 140-153. doi:10.1016/j.jconhyd.2008.05.008

Chapman, S. M. and B. Parker. *High Resolution Field Characterization and Numerical Modeling for Analysis of Contaminant Storage and Release from Lower Permeability Zones*. SERDP, 2011.

Christ, J.A., L.D. Lemke, and L.M. Abriola (2005), Comparison of two-dimensional and three-dimensional simulations of dense non-aqueous phase liquids (DNAPLs): Migration and entrapment in a nonuniform permeability field, *Water Resources Research*, 41, W01007. doi: 10.1029/2004WR003239.

Christ, J. A., C. A. Ramsburg, K.D. Pennell, and L.M. Abriola (2006). Estimating mass discharge from dense nonaqueous phase liquid source zones using upscaled mass transfer coefficients: An evaluation using multiphase numerical simulations. *Water Resources Research*, 42(11), W11420, doi:10.1029/2006WR004886

Christ, J. A. Personal Correspondence. 7 March 2014.

Clement, T. P., Gautam, T. R., Lee, K K., Truex, M. J., Davis, G. B. (2004). Modeling of DNAPL-Dissolution, Rate-Limited Sorption and Biodegradation Reactions in Groundwater Systems. *Bioremediation Journal*, 8 (1-2): 47-64. doi: 10.1080/10889860490453177

Demond, A.H. Impact of Chlorinated Solvents on the Structure of Clay in Low Permeability Zones in Groundwater Contamination Source Areas, Presentation Delivered at Partners in Environmental Technology Technical Symposium and Workshop, Washington DC, 30 November-2 December 2010.

EPA Superfund Record of Decision: Fort Lewis Logistics Center (1990) [online]. [Accessed 10 February 2014]. Available from World Wide Web: <http://www.epa.gov/superfund/sites/rods/fulltext/r1090025.pdf>

EPA Explanation of Significant Differences: Fort Lewis Logistics Center (1998) [online]. [Accessed 13 February 2014]. Available from World Wide Web: <http://www.epa.gov/superfund/sites/rods/fulltext/e1098040.pdf>

InsideEPA.com. "EPA Seeks To Ease Groundwater Cleanup Policy Following NAS Report," *Inside EPA Public Content*. 34 (38): 1-3 [online]. [Accessed 23 September 2013]. Available from World Wide Web: <http://insideepa.com/Inside-EPA-General/Inside-EPA-Public-Content/epa-seeks-to-ease-gr>

The Interstate Technology & Regulatory Council. (ITRC) (2010)"Use and Measurement of Mass Flux and Mass Discharge" [online] [Accessed 6 Jan 2013]. Available from World Wide Web:

http://www.cluin.org/download/contaminantfocus/dnapl/Detection_and_Site_Characterization/DNAPL-Mass-flux-1.pdf

EPA. *Basic Information about Regulated Drinking Water Contaminants*. [online]. [Accessed 15 May 2013]. Available from World Wide Web:
<<http://water.epa.gov/drink/contaminants/basicinformation/trichloroethylene.cfm>>

Huang, J. Personal Correspondence. 17 October 2013.

Kueper, B. H., and Davies, K. L. (2009) Ground water issue. *Assessment and Delineation of DNAPL Source Zones at Hazardous Waste Sites*. [online]. [Accessed 13 September 2013]. Available from World Wide Web:
<<http://nepis.epa.gov/Adobe/PDF/P1006Y98.pdf>>

Minitier, J. M., *Modeling Enhanced Storage of Groundwater Contaminants Due to the Presence of Cracks in Low Permeability Zones Underlying Contaminant Source Areas*. MS thesis, AFIT/GES/ENV/11-M02. Graduate School of Engineering and Management, Air Force Institute of Technology (AU), Wright-Patterson AFB OH, March 2011.

National Research Council of the National Academies (NRC). *Alternatives for Managing the Nation's Complex Contaminated Groundwater Sites*. Washington D.C. , 2012. [online]. [Accessed 24 September 2013]. Available from World Wide Web:
http://www.nap.edu/catalog.php?record_id=14668

Oolman, T. (1995). DNAPL flow behavior in a contaminated aquifer: Evaluation of field data. *Ground Water Monitoring & Remediation*, 15(4), 125; 125-137; 137.

Parker, B.L., S. W. Chapman, and M. A. Guilbeault. (2008). Plume Persistence Caused by Back Diffusion from Thin Clay Layers in a Sand Aquifer Following TCE Source-Zone Hydraulic Isolation. *Journal of Contaminant Hydrology*. 102(1-2): 86-104.

Parker, B.L., J.A. Cherry, and S. W. Chapman. (2004). Field Study of TCE diffusion profiles below DNAPL to assess aquitard integrity. *Journal of Contaminant Hydrology*. 74 (1-4): 197-230.

Sale, T. C., & McWhorter, D. B. (2001). Steady state mass transfer from single-component dense nonaqueous phase liquids in uniform flow fields. *Water Resources Research*, 37(2), 393-404. doi:10.1029/2000WR900236

Sievers, K.W. *Modeling the Impact of Cracking In Low Permeability Layers In a Groundwater Contamination Source Zone On Dissolved Contaminant Fate and Transport*. MS thesis, AFIT/GES/ENV/12-M02. Graduate School of Engineering and Management, Air Force Institute of Technology (AU), Wright-Patterson AFB OH, March 2012.

Yang, Z., Niemi, A., Fagerlund, F., & Illangasekare, T. (2012). Effects of single-fracture aperture statistics on entrapment, dissolution and source depletion behavior of dense non-aqueous phase liquids. *Journal of Contaminant Hydrology*, 133(0), 1-16. doi:10.1016/j.jconhyd.2012.03.002

Zhu, J., & Sykes J. F. (2003). Simple screening models of NAPL dissolution in the subsurface. *Journal of Contaminant Hydrology*, 72 (0), 245-258. doi: 10.1016/j.jconhyd.2003.11.002

| | | | | | | |
|---|-------------|-----------------------|---------------------------------------|------------------------------------|---|--|
| REPORT DOCUMENTATION PAGE | | | | | <i>Form Approved OMB No. 0704-0188</i> | |
| <small>The public reporting burden for this collection of information is estimated to average 1 hour per response, including the time for reviewing instructions, searching existing data sources, gathering and maintaining the data needed, and completing and reviewing the collection of information. Send comments regarding this burden estimate or any other aspect of this collection of information, including suggestions for reducing the burden, to Department of Defense, Washington Headquarters Services, Directorate for Information Operations and Reports (0704-0188), 1215 Jefferson Davis Highway, Suite 1204, Arlington, VA 22202-4302. Respondents should be aware that notwithstanding any other provision of law, no person shall be subject to any penalty for failing to comply with a collection of information if it does not display a currently valid OMB control number.</small> | | | | | | |
| PLEASE DO NOT RETURN YOUR FORM TO THE ABOVE ADDRESS. | | | | | | |
| 1. REPORT DATE (DD-MM-YYYY) | | 2. REPORT TYPE | | | 3. DATES COVERED (From - To) | |
| 4. TITLE AND SUBTITLE | | | | 5a. CONTRACT NUMBER | | |
| | | | | 5b. GRANT NUMBER | | |
| | | | | 5c. PROGRAM ELEMENT NUMBER | | |
| 6. AUTHOR(S) | | | | 5d. PROJECT NUMBER | | |
| | | | | 5e. TASK NUMBER | | |
| | | | | 5f. WORK UNIT NUMBER | | |
| 7. PERFORMING ORGANIZATION NAME(S) AND ADDRESS(ES) | | | | | 8. PERFORMING ORGANIZATION REPORT NUMBER | |
| 9. SPONSORING/MONITORING AGENCY NAME(S) AND ADDRESS(ES) | | | | | 10. SPONSOR/MONITOR'S ACRONYM(S) | |
| | | | | | 11. SPONSOR/MONITOR'S REPORT NUMBER(S) | |
| 12. DISTRIBUTION/AVAILABILITY STATEMENT | | | | | | |
| 13. SUPPLEMENTARY NOTES | | | | | | |
| 14. ABSTRACT | | | | | | |
| 15. SUBJECT TERMS | | | | | | |
| 16. SECURITY CLASSIFICATION OF: | | | 17. LIMITATION OF ABSTRACT | 18. NUMBER OF PAGES | 19a. NAME OF RESPONSIBLE PERSON | |
| a. REPORT | b. ABSTRACT | c. THIS PAGE | | | 19b. TELEPHONE NUMBER (Include area code) | |